

Improving Efficiency of Metabolic Flux Sampling via Monte-Carlo Algorithm: From Network Preprocessing to the Emergence of Bypass Pathways

Lu Xie^{*#}, Yi Zhang^{*#}

^{*}School of Life Science, University of Science and Technology of China, Hefei, Anhui, P. R. China.

[#]These people contribute equally to this work.

Abstract

Constraint-based modeling is a widely used approach to analyze metabolic networks which were reconstructed from variety of biological data. The linear constraints, such as thermodynamic feasibility constraint, mass conservation constraint and capacity constraint, can be imposed hands down in the linear programming or uniform random sampling. But recently, a non-linear constraint, known as “loop law”, is challenging the existing algorithms. Here we present a more simple and efficient sampling method which contains three steps: (1) Network preprocessing: pick up the non-zero flux excluding the zero flux to decrease the rows of the stoichiometric matrix, and discover the latent loops of the network by linear programming; (2) Sampling the flux space: sample the null space of the stoichiometric matrix using Simulated Annealing Monte-Carlo method with a potential energy function which we defined to enforce additional constraints mentioned above, including the virtual chemical potential constraint (VCPC for short) to apply the loop-law; (3) Checking results: inspect that whether the samples have loop flux or not by solving an inequality. In addition, we pointed out a new type of pathways: the bypass pathways, which have exchange flux with environment but are independent to the biomass synthesis. Albeit their biological functions are not revealed yet, here we present a linear programming based method for eliminating the bypass fluxes (EBF for short). We employed these methods to analysis the genome-scale metabolic network of *Helicobacter pylori*.

Keywords: constraint-based, loop law, Simulated Annealing Monte-Carlo.

1. Introduction

A growing number of genome-scale metabolic networks have been reconstructed by using multiple different data types(1-4). Current theories have various strengths and shortcomings in analyzing these biochemical networks. Specifically, dynamic mathematical modeling of large-scale networks meets difficulties because the necessary mechanistic details and kinetic parameters are rarely available. Thus, more efficient modeling techniques are required, such as constraint-based approaches(5, 6). Flux Balance Analysis (FBA)(7) , which is based on the steady state hypothesis. In this hypothesis all metabolites in a metabolic network do not change in quantities, and the network is mass-balanced. The varieties of the metabolites are calculated as follows:

$$\frac{dX}{dt} = S \cdot v \quad (1)$$

Where X denotes the quantities of the metabolites, and S denotes the stoichiometric matrix, v denotes the vector of a set of fluxes. When on steady-state:

$$\frac{dX}{dt} = 0 \Rightarrow S \cdot v = 0 \quad (2)$$

$$v = (v_1, \dots, v_n)'$$

$$X = (X_1, \dots, X_m)'$$

In this approach we can impose some constraints of identifiable physicochemical laws on a metabolic network to form a solution space, the steady-state flux space. These constraints are familiar, such as mass conservation constraint, thermodynamic feasibility constraints and so on, which are all linear constraints. For a specific system, a steady-state flux space is defined by these linear constraints, which always lead to the definition of the convex solution space, so linear programming can be used to predict the lethality of knockouts(8), optimal growth rates(9) and ranges of achievable fluxes(10). Uniform random sampling of these convex solution spaces can determine the range and the shape of possible steady-state fluxes distributions allowed in the network under defined physicochemical constraints(11). It has been utilized widely, such as finding a “high-flux backbone” in *Escherichia coli* metabolism(12),

researching the effect of enzymopathies in human red blood cells(13). But recently, Beard, Qian and their colleagues' work(14, 15) have pioneered one of the thermodynamic constraints, the loop law. Two basic laws of thermodynamics lead to this constraint. First, the sum of chemical potentials around a loop must equal zero:

$$\sum_{i \in \text{loop}} \Delta\mu_i = 0 \quad (3)$$

Second, all of the reactions must follow the downward direction of the chemical potentials:

$$v_i \cdot \Delta\mu_i \leq 0 \quad \forall i \quad (4)$$

When these two equations can be satisfied simultaneously, the net flux around a biochemical loop must be equal to zero, resulting in the “loop law” for reaction fluxes. Because of its non-linear characteristic, some common sampling methods became inefficient. Palsson and his colleagues have designed a four step sampling method(16), which can solve this question. Herein we present a three step sampling method can integrate all the constraints mentioned above conveniently. We adopt the genome-scale metabolic network of *H. pylori* (iT341 GSM/GPR)(2) as an example to illustrate this method. The sampling space has also been proven to be convergent. All of the programs were implemented on the MATLAB 7.0.

2. Material and methods

2.1 System and Model

H. pylori is a kind of notorious human gastric pathogen, which infects almost half of the world population. Palsson and his colleagues have reconstructed the *H. pylori* strain 26695's metabolic network based on the revised genome annotation and new experimental data in 2005(2). That is iT341 GSM/GPR, the genome-scale metabolic model. It integrated the biochemical and genomic data and contains the reactions catalyzed by the enzymes associated genes. In total, iT341 GSM/GPR accounts for 341 metabolic genes, 476 internal reactions, 74 external reactions, 8 demand functions, 411 internal metabolites and 74 external metabolites. Demand functions are the reactions of the type: A -->; this means that the compound A can be only produced by

the network, without further balancing the compound A, including a biomass function, a HMFURN function, demand functions for thiamin, menaquinone 6, biotin and heme (protoheme), sinking reactions for ahcys(c) and amob. So the stoichiometric matrix S has 558 reactions and 485 metabolites.

2.2 Network Preprocessing

2.2.1 Discover the Latent Loops

At first we eliminated 74 external reactions and 8 demand functions via knocking out corresponding column vectors of the stoichiometric matrix S in order to make sure the system closed. Then a linear programming (called LP1 later) was used to find the maximum and minimum allowable flux on the remained reactions(10).

$$\begin{aligned} & \max \text{ and } \min v_i; i = 1, 2, \dots, n \\ & \text{such that } \begin{cases} S_{ko} \times v = 0 \\ -10 < v_i < 10, \forall i \in \text{reversible reactions} \\ 0 < v_i < 10, \forall i \in \text{irreversible reactions} \end{cases} \end{aligned} \quad (5)$$

Here S_{ko} is the stoichiometric matrix with knockouts. The upper and lower limits for reversible reactions are 10 and -10 while 10 and 0 for irreversible ones, respectively. From the results, most fluxes are constrained to be zero while a few ones are not (Fig. 2 A). These non-zero reactions could construct loops in the network.

2.2.2 Eliminating the Zero Reactions

After calculating the maximum and the minimum values of every flux by linear programming(10), without knockouts, we can observe that some fluxes are always equal to zero, because these reactions contain dead-end metabolites(2). Deleting these reactions would be the best choice because of their invalidation and the opportunity to shrink the sampling space.

2.3 Monte-Carlo sampling

2.3.1 Definition of the Potential Energy Function

We assumed the possible steady-states as a thermodynamics ensemble and defined the

potential energy function(17). This function is used to construct the profile of the solution space, not decides the distributions of the fluxes in the solution space.

$$E = E_1 + E_2 \quad (6)$$

$$E_1 = \sum_{i=1}^n e_i; e_i = \begin{cases} (\alpha_i - v_i)^2; & \text{when } v_i < \alpha_i \\ (v_i - \beta_i)^2; & \text{when } v_i > \beta_i \\ 0; & \text{otherwise} \end{cases} \quad (7)$$

$$E_2 = \sum_i \left(\frac{|v_i \cdot \Delta\mu_i| + v_i \cdot \Delta\mu_i}{2} \right)^2, \forall i \in \text{loop reactions} \quad (8)$$

While:

$$\Delta\mu = \mu^T \times S_{loop} \quad (9)$$

Here, n is the number of reactions, v_i denotes the flux of the metabolic reactions and $\Delta\mu_i$ denotes the change of chemical potential. Eq. 7 is a penalty term to impose the capacity constraint on the reactions, in which α_i and β_i are lower and upper limits for each reaction, respectively. For irreversible reactions, α_i was set to zeros, whereas β_i were usually set to either measured uptake rates for transport reactions or the v_{max} of the corresponding enzymes. Here we set the α_i and β_i to -10 and 10 for reversible reactions while 0 and 10 for irreversible ones, which is given consideration to the number of sampling steps and step size. Eq. 8 is aiming at imposing the thermodynamic constraints(14, 15). Column vector μ is hypothesized to be a set of virtual chemical potentials for the metabolites in the loop reactions, and S_{loop} is a subset of stoichiometric matrix, which is composed by reactions and metabolites all from the internal loops.

2.3.2 The Sampling Space

In truth, there are sets of fluxes satisfying these constraints, all of which make up of a solution space. But the dimensions are too large for sampling, so we will sample the solution space via sampling the null space of the stoichiometric matrix. Every row vector of N is a base vector of the solution space and N satisfies:

$$S \cdot N^T = 0 \quad (10)$$

The constraints imposed by the solution space will be converted to the null space. In next section we will prove that the profile of the null space is as same as the solution space.

2.3.3 The Sampling Steps

The system evolves from a kinetic Metropolis Monte-Carlo(11, 18) and has 3 steps:

Step1: At the beginning, we choose a set of random coefficients c as starting point.

Then we can get a initial set of fluxes v :

$$v = c \times N; \quad c \in [0,1] \quad (11)$$

Step2: Randomly choose a coefficient c_i from c_1, \dots, c_n , and perturb c_i by increase or decrease a random value between $[0, 0.2]$.

Step3: Calculate the energy term before and after the perturbation, and get the difference:

$$\Delta E = E_{after} - E_{before} \quad (12)$$

The acceptance rate is given as:

$$p = \exp\left(\frac{-\Delta E}{T}\right) \quad (13)$$

Here T is the temperature coefficient but has no physical signification. In every evolvment we perturb one parameter and calculate ΔE . If $\Delta E > 0$ the new parameters will be accepted, else will be accepted by rate p . Hence, we set T small enough to insure that the rate will fall down remarkably if the constraints are broken and the parameters will hardly be accepted anyway.

2.3.4 Pre-sampling

Upon the pre-sampling in the solution space, it was found that the Eq. 5 is always not equal to zero. That means the thermodynamics constraint was always violated. After checking the samples, we found the reaction AHSERL2's flux was nearly forced to zero. We can infer that the loop containing the AHSERL2 is irrational, because all of the reactions were under systemic constraints that forced them to be irreversible in the directions that formed the loop(16). Therefore, we delete it from the network.

2.4 Eliminating the Bypass Flux (EBF)

We also ameliorate the LP1 algorithm in order to define a new type of pathways: bypass pathways, which are not internal but do not contribute to biomass synthesis, as Fig. 1. The amelioration is to knock out only the biomass synthesis reaction. Some of these bypass reactions can only be constrained by the maximum and minimum flux boundaries, as Fig. 2 B. Their fluxes could fluctuate freely between the upper and lower limit in defiance of the biomass production, demonstrating the same as the loop fluxes.

We developed a linear programming based algorithm to eliminate the bypass flux in the samples obtained from the Monte-Carlo sampling:

$$\begin{aligned} & \text{Min}(\sum_i \text{abs}(v_i)), \forall i \in \text{bypass reactions} \\ & \text{such that } \begin{cases} S \times v = 0 \\ -10 < v_i < 10, \forall i \in \text{reversible reactions} \\ 0 < v_i < 10, \forall i \in \text{irreversible reactions} \end{cases} \end{aligned}$$

3. Result and Discussion

3.1 The Latent Loops

First we presented the LP1 algorithm, with which we can find out all the specific reactions that could be combined in internal loops (as Fig. 2 A), faster than with analyzing extreme pathways(19, 20). In the original network we discovered 22 latent loop reactions, belonging to 6 internal loops. 4 of these loops are presented in previous works(16), and the other 2 are shown in Fig. 3. The Fig. 3 A is equivalent to a single irreversible reaction. However, the 2 loops are both isolated from the mainstream of the network; hence they are deleted in our modified network.

3.2 The Monte-Carlo Sampling

3.2.1 The Sample Sets

In the next step, we performed a uniform Monte-Carlo sampling in the steady state flux space. The sampling is not only constrained by the irreversible constraint but also

by the VCPC on the latent loop reactions that discovered in the first step. Because the particular upper/lower limit of each flux is insufficient, the upper/lower limit is artificially set to 10/-10 for reversible reactions, and 10/0 for irreversible ones, respectively. We recorded 10 sample sets with VCPC and another 10 sample sets without the constraint. 2,000 samples were recorded for each sample set with random starting point, while the samples are recorded every 1,000 steps. We discarded all of the beginning samples whose potential energies were not equal to zero to ensure that the samples did not violate any of the constraints.

3.2.2 *The Null Space of Stoichiometric Matrix*

The solution space is circumscribed by the extreme pathways, act as its edge. Conventional sampling usually treat extreme pathways as base vectors, but the number of extreme pathways is too immense for sampling. So we use constraint based null space of stoichiometric matrix, N , as our sampling space, and treat the rows of N as base vectors. For this network, the null space has 89 row vectors, which is feasible for sampling. For any two vectors in null space:

$$v_1 = c_1 \cdot N$$

$$v_2 = c_2 \cdot N$$

Where vectors v_1 and v_2 denotes any sets of fluxes in the solutions space. For any combination of the two vectors:

$$\lambda \cdot v_1 + (1 - \lambda) \cdot v_2; (0 \leq \lambda \leq 1)$$

This can always be transformed into:

$$(\lambda \cdot c_1 + (1 - \lambda) \cdot c_2) \cdot N; (0 \leq \lambda \leq 1)$$

So the combined vector is also in the null space, which means that if the solution space is a convex cone then the null space is also a convex cone.

3.2.3 *The Consistency of Sampling Space*

The Principal Component Analysis (PCA) on the covariance matrix of each sample set reveals that the 20 eigenvectors corresponding to the 20 maximum eigenvalues

could characterize approximately 99% variance of the flux space. To test the consistency of sampling space we calculated the Root Mean Square Inner Product (RMSIP)(21) between the eigenvectors of sample sets with different start points:

$$RMSIP = \sqrt{\frac{1}{n} \sum_{i=1}^n \sum_{j=1}^n (C_{A,i} \times C_{B,j}^T)^2} \quad (14)$$

While n is the number of eigenvectors and here n is 20. $C_{A,i}$ and $C_{B,j}$ are the eigenvectors (row vectors) from two different samples A and B. The results are fairly acceptable (see Table 1), which reflect the overlapping degrees of different sampling spaces and the ideal value is 1.

3.3 The Effect of Our Constraint Based Sampling

All the 15 loop flux's distribution comparisons between the sample sets with and without VCPC are shown in Fig. 4. To validate that our method can avoid the appearance of loop fluxes in the samples, we developed an algorithm to inspect the samples by solving the inequality:

$$A^T \times \mu \leq 0 \quad (15)$$

While:

$$A_{i,j} = S_{i,j} \cdot v_j \quad (16)$$

Here S is the stoichiometric matrix, v is the vector of flux from the samples, and unknown vector μ represents the virtual chemical potential of the metabolites. If this inequality is solvable, we can find a set of suitable potentials for all metabolites that satisfies the VCPC:

$$\Delta\mu \times v \leq 0 \quad (17)$$

While:

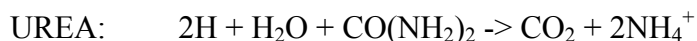
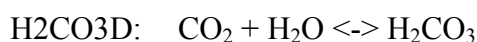
$$\Delta\mu = \mu^T \times S \quad (18)$$

On the contrary, when a sample contains loop flux, we can never find a suitable potential set to satisfy Eq. 15. By employing this algorithm, we find no loop flux in our Monte-Carlo samples, which indicates that only constraining loop reactions with

VCPC is effective on avoiding the appearance of loop flux. Further more, we also adopt this algorithm to verify the samples of other metabolic networks that cannot form any internal loops, while the sampling progress is not constrained by VCPC. The result is that Eq. 15 is always solvable, which indicates that it is not necessary to constrain the reactions that cannot form internal loops. This conclusion is important especially for large scale metabolic networks with hundreds of metabolites, because if we have to assign a virtual potential to each metabolite, the sampling space will expand exponentially and the Monte –Carlo method will become infeasible. Now we only have to assign virtual potentials to the metabolites which are involved in the loop-forming reactions, and these reactions could be discovered in the first place.

3.4 The Effect of EBF

We selected two typical bypass reactions to testify the effect of EBF:



All these reactants are exchangeable, which means that they could be transported across the membrane freely. After the processing of EBF, their flux distributions are constrained closely to zero (Fig. 5). We also calculated the RMSIP of the sample sets after the processing of EBF (Table 1).

To sum up, in this paper we provided a series of methods with 3 steps: (1) Discovering latent internal loops in a metabolic network; (2) Avoiding the appearance of loop flux in the procedure of sampling by the thermodynamic constraint; (3) Inspecting the samples for containing internal loop flux or not. Based on the linear program the step (1) are faster than using extreme pathways. The results of step (3) validate our approach of imposing the thermodynamic constraint on Monte-Carlo sampling and this approach is generally applicable to all metabolic networks. In addition we pointed out the emergence of bypass pathways, but their biological functions and the significance of their existence are not discussed in this place.

Reference

1. Duarte, N. C., M. J. Herrgard, and B. O. Palsson. 2004. Reconstruction and validation of *Saccharomyces cerevisiae* iND750, a fully compartmentalized genome-scale metabolic model. *Genome research* 14:1298-1309.
2. Thiele, I., T. D. Vo, N. D. Price, and B. O. Palsson. 2005. Expanded metabolic reconstruction of *Helicobacter pylori* (iT341 GSM/GPR): an in silico genome-scale characterization of single- and double-deletion mutants. *J Bacteriol* 187:5818-5830.
3. Francke, C., R. J. Siezen, and B. Teusink. 2005. Reconstructing the metabolic network of a bacterium from its genome. *Trends Microbiol* 13:550-558.
4. Feist, A. M., C. S. Henry, J. L. Reed, M. Krummenacker, A. R. Joyce, P. D. Karp, L. J. Broadbelt, V. Hatzimanikatis, and B. O. Palsson. 2007. A genome-scale metabolic reconstruction for *Escherichia coli* K-12 MG1655 that accounts for 1260 ORFs and thermodynamic information. *Molecular systems biology* 3:121.
5. Price, N. D., J. A. Papin, C. H. Schilling, and B. O. Palsson. 2003. Genome-scale microbial in silico models: the constraints-based approach. *Trends Biotechnol* 21:162-169.
6. Price, N. D., J. L. Reed, and B. O. Palsson. 2004. Genome-scale models of microbial cells: evaluating the consequences of constraints. *Nature reviews* 2:886-897.
7. Amit Varma, and B. O. Palsson. 1994. Metabolic Flux Balancing: Basic Concepts, Scientific and Practical Use. *Bio/Technology* 12:994-998.
8. Forster, J., I. Famili, B. O. Palsson, and J. Nielsen. 2003. Large-scale evaluation of in silico gene deletions in *Saccharomyces cerevisiae*. *Omics* 7:193-202.
9. Edwards, J. S., R. U. Ibarra, and B. O. Palsson. 2001. In silico predictions of *Escherichia coli* metabolic capabilities are consistent with experimental data. *Nature biotechnology* 19:125-130.
10. Mahadevan, R., and C. H. Schilling. 2003. The effects of alternate optimal solutions in constraint-based genome-scale metabolic models. *Metabolic engineering* 5:264-276.
11. Wiback, S. J., I. Famili, H. J. Greenberg, and B. O. Palsson. 2004. Monte Carlo sampling can be used to determine the size and shape of the steady-state flux space. *J Theor Biol* 228:437-447.
12. Almaas, E., B. Kovacs, T. Vicsek, Z. N. Oltvai, and A. L. Barabasi. 2004. Global organization of metabolic fluxes in the bacterium *Escherichia coli*. *Nature* 427:839-843.
13. Thiele, I., N. D. Price, T. D. Vo, and B. O. Palsson. 2005. Candidate metabolic network states in human mitochondria. Impact of diabetes, ischemia, and diet. *The Journal of biological chemistry* 280:11683-11695.
14. Beard, D. A., S. D. Liang, and H. Qian. 2002. Energy balance for analysis of complex metabolic networks. *Biophys J* 83:79-86.
15. Beard, D. A., E. Babson, E. Curtis, and H. Qian. 2004. Thermodynamic constraints for biochemical networks. *J Theor Biol* 228:327-333.
16. Price, N. D., I. Thiele, and B. O. Palsson. 2006. Candidate states of *Helicobacter pylori*'s genome-scale metabolic network upon application of "loop law" thermodynamic constraints. *Biophys J* 90:3919-3928.
17. Brown, K. S., C. C. Hill, G. A. Calero, C. R. Myers, K. H. Lee, J. P. Sethna, and R. A. Cerione. 2004. The statistical mechanics of complex signaling networks: nerve growth factor signaling. *Physical biology* 1:184-195.

18. Nicholas Metropolis, A. W. R., Marshall N. Rosenbluth, and Augusta H. Teller 1953. Equation of State Calculations by Fast Computing Machines. 21:1087-1092
19. Price, N. D., I. Famili, D. A. Beard, and B. O. Palsson. 2002. Extreme pathways and Kirchhoff's second law. *Biophys J* 83:2879-2882.
20. Bell, S. L., and B. O. Palsson. 2005. Expa: a program for calculating extreme pathways in biochemical reaction networks. *Bioinformatics* 21:1739-1740.
21. de Groot, B. L., D. M. van Aalten, A. Amadei, and H. J. Berendsen. 1996. The consistency of large concerted motions in proteins in molecular dynamics simulations. *Biophys J* 71:1707-1713.

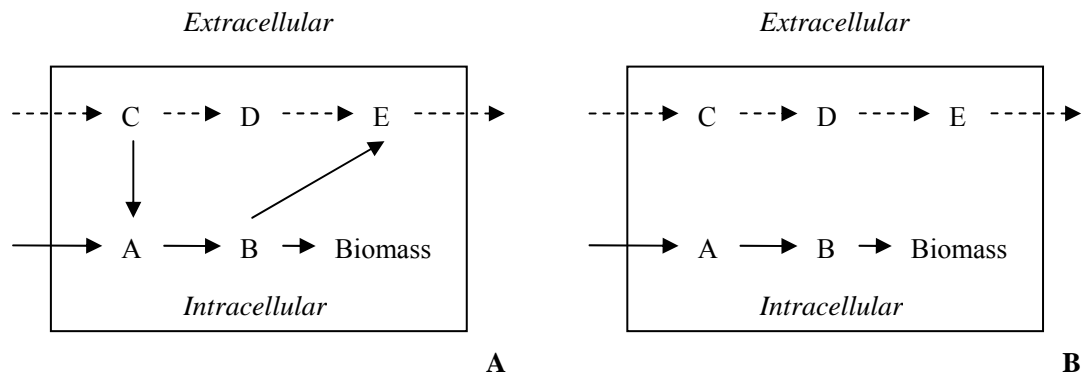
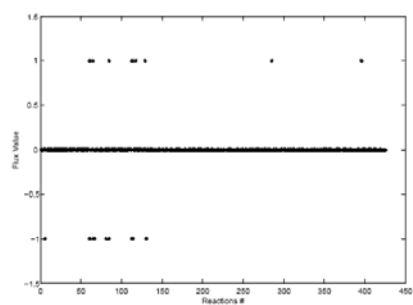
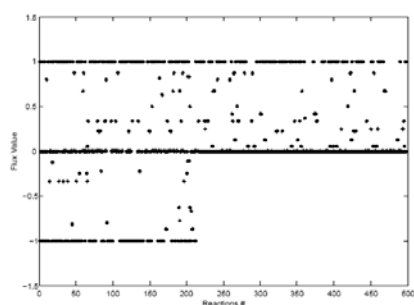


Fig. 1

Two sketch maps of bypass pathways, which are indicated by the dotted arrows. These bypass pathways could be either partially linked (A) with or completely separate (B) from the mainstream of biomass synthesis.



A



B

Fig. 2

- B. The result of linear programming with knocking the biomass synthesis and exchange reactions out of the original stoichiometric matrix.
- C. The result of linear programming with knocking only the biomass synthesis reaction out of the modified stoichiometric matrix.

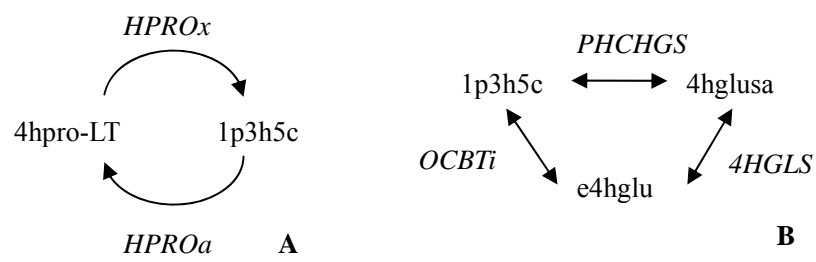


Fig. 3

The 2 out of 6 internal loops discovered in the original network.

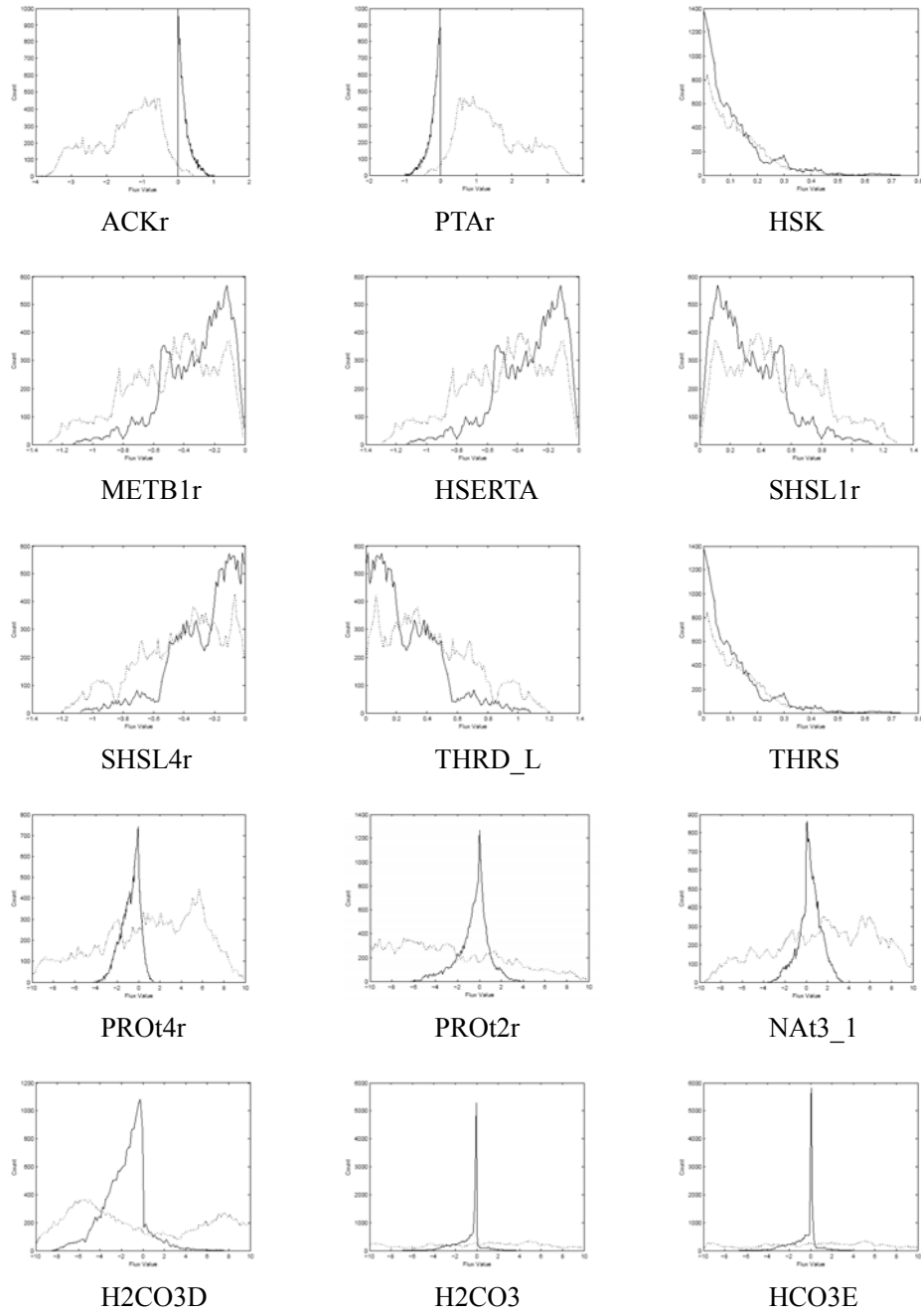
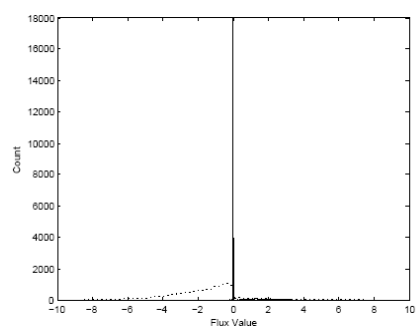
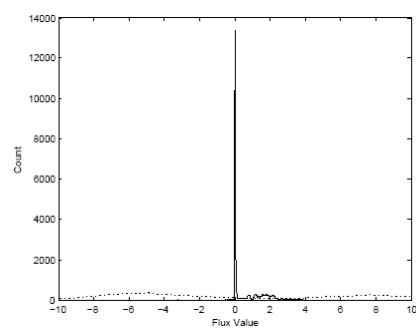


Fig. 4

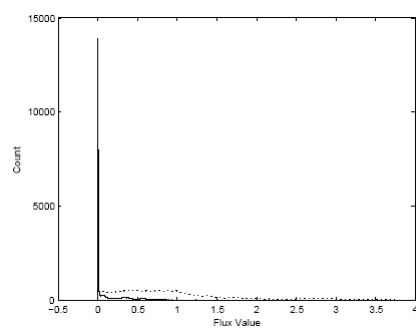
The flux distributions of all 15 loop reactions illustrate the effect of VCPC. The dotted lines indicate the distributions of samples without VCPC and the solid lines indicate the distributions of samples with VCPC.



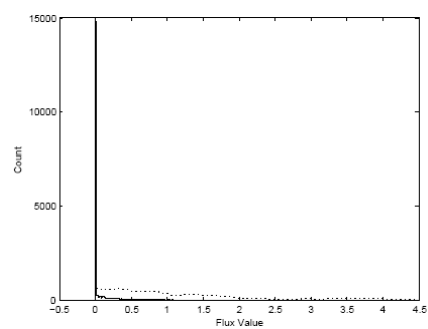
H₂CO₃D, with VCPC



H₂CO₃D, without VCPC



UREA, with VCPC



UREA, without VCPC

Fig. 5

The flux distributions of two bypass reactions (H₂CO₃D and UREA) illustrate the effect of EBF. The dotted lines indicate the distributions of original samples and the solid lines indicate the distributions of EBF-processed samples.

Table 1. The RMSIP value among 10 sample sets

Mean Value	Variance	With VCPC	With EBF
0.8693	8.573E-5	No	No
0.8553	2.357E-4	Yes	No
0.8109	1.232E-3	No	Yes
0.8104	2.139E-3	Yes	Yes